Inorganic Chemistry

ARTICLE

pubs.acs.org/IC

# Spin Canting and Metamagnetism in 2D and 3D Cobalt(II) Coordination Networks with Alternating Double End-On and Double End-to-End Azido Bridges

Jaursup Boonmak,[†] Motohiro Nakano,[‡] Narongsak Chaichit,[§] Chaveng Pakawatchai,[∥] and Sujittra Youngme*[,†]

[†]Department of Chemistry and Center of Excellence for Innovation in Chemistry, Faculty of Science, Khon Kaen University, Khon Kaen 40002, Thailand

[‡]Division of Applied Chemistry, Graduate School of Engineering, Osaka University, Suita, Osaka 565-0871, Japan

[§]Department of Physics, Faculty of Science and Technology, Thammasat University Rangsit, Pathumthani 12121, Thailand

[∥]Department of Chemistry, Faculty of Science, Prince of Songkla University, Hat Yai, Songkla 90112, Thailand

Supporting Information

**ABSTRACT:** By employing an *N,N′*-ditopic spacer 2-aminopyrazine (ampyz), two-dimensional (2D) (**1**) and three-dimensional (3D) (**2**) azido-bridged cobalt(II) coordination networks with the identical formula $[Co(N_3)_2(ampyz)]_n$ have been synthesized and characterized structurally and magnetically. Compound **1** was prepared by the layer diffusion method in ambient temperature and crystallized in the high symmetric space group *Immm*. The 2D square-grid structure of **1** contains the perfect symmetric linear of alternating double end-on (EO) and double end-to-end (EE) azido-bridged $Co^{II}$ chains which are linked together by an ampyz spacer in *trans*-arrangement. The intralayer $\pi-\pi$ stacking interactions among ampyz spacers additionally stabilize this layer. The adjacent 2D layers are assembled by the intermolecular hydrogen bonding between the $NH_2$ of the ampyz and the EE azido ligands building a 3D structure. Compound **2** was prepared by a hydrothermal technique and shows a 3D framework containing a zigzag chain of similarly alternating double EO and double EE azido-bridged $Co^{II}$ center. In contrast, this chain is linked by two ampyz spacers in *cis*-fashion giving rise to a 3D structure. The magnetic investigation of **1** shows the coexistence of a big spin canting angle and metamagnetism having magnetic ordering at 10 K, whereas the magnetic behavior of **2** simply exhibits spin-canted antiferromagnetism below $T_N$ of 16 K.

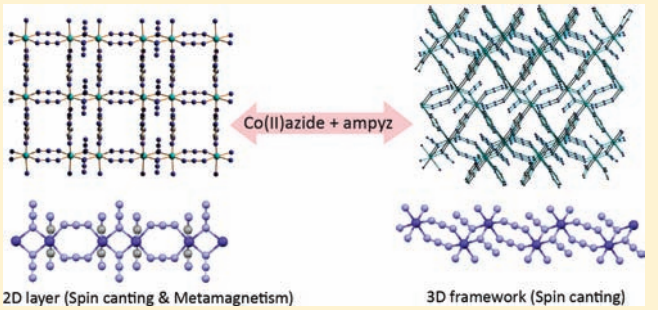


## INTRODUCTION

The crystal engineering and magnetism of molecule-based coordination frameworks with low- or high dimensional structures have been of great interest in recent years with the intention of understanding the fundamental magneto-structural correlations within the structure and controlling the spins in molecules and molecular assemblies for conceiving practical functional molecule-based materials.[1−5] To rationally design magnetic molecular assemblies, it is important to select the appropriate bridging ligands that effectively transmit the exchange interactions between the spin carriers together with the aspects of diverse topologies. An excellent azido ligand is the one of the extensively used bridging ligands in the construction of magnetic molecular materials because it can provide a short bridge with the extremely versatile coordination modes and effectively mediates either ferromagnetic or antiferromagnetic coupling generally through $\mu_2$-1,1 (end-on, EO) and $\mu_2$-1,3 (end-to-end, EE) modes, respectively. In addition the different combinations of EO and EE azido bridging modes may exist in the same structure, leading to several topologies as well as competing magnetic interactions in sign according to a certain EO and EE azido bridging sequence.[6−12] Consequently, the fascinating magnetic phenomena have been recognized in many azido-bridged coordination polymers which have been an active research area so far.[6,13−15] Likewise, the organic coligands are very significant to the formation of some particular architectures and to their structural modification. It is well-known that the *N,N′*-ditopic diimine spacer pyrazine (pyz) is a long bridge for magnetic systems and effectively transfers electrons in the antiferromagnetic superexchange pathways between metal centers. With pyz and derivatives of pyz ligands, the azido complexes usually exhibit various structural topologies together with interesting magnetic properties.[16−20] For instance, the 2D layer of $[Fe(N_3)_2(pyz)]_n$ showed metamagnetism arising from the competition of ferromagnetically coupled EO azido chains and 2D antiferromagnetically coupling via pyz.[18] In

**Received:** May 17, 2011
**Published:** July 05, 2011

  

contrast with the lack of local anisotropic ions, this metamagnetic feature for the $Mn^{II}$ and $Cu^{II}$ analogues was not observed.[19,20]

In this report, we are interested in the versatile 2-aminopyrazine (ampyz) spacer as organic coligand in a magnetic azido complex system. The ampyz spacer contains many interaction sites; coordination sites at the N atoms on the pyrazine ring, hydrogen donor sites at the amino group, and the intermolecular $\pi-\pi$ stacking site through aromatic moieties, which has been used for constructing many coordination polymers.[21−25] Without the spin carriers, the structural diversity of zinc(II) azido complexes with ampyz has been recently obtained depending on the molar ratio of the starting components.[24] With this in mind, herein we show that the ampyz spacer accommodates well in the magnetic anisotropic $Co^{II}$ azido system. Remarkably, new 2D layer (**1**) and 3D framework (**2**) of azido-bridged $Co^{II}$ coordination networks with the identical molar ratio $[Co(N_3)_2(ampyz)]_n$ were well prepared in different preparative techniques and characterized structurally and magnetically. In addition both complexes similarly contain the 1D chain of alternately double EO and double EE azido-bridged $Co^{II}$ ions, whereas the ampyz spacers in **1** and **2** are in dissimilar arrangements, *trans*- and *cis*-positions in octahedral $Co^{II}$ ions for **1** and **2**, respectively. To our knowledge, only two azido $Co^{II}$ chains with alternating double EE and double EO bridges have been reported in the literature.[26,27] Although **1** and **2** are similar in local coordination environments, they are somewhat different in structural symmetries, dimensionalities, and bridging parameters; consequently, their magnetic behaviors at low temperature reveal the significant disparities. Complex **1** exhibits complex magnetic behaviors combining a big spin canting angle and metamagnetism while **2** simply displays the canted antiferromagnetism with a smaller canting angle. These behaviors allow us to perform the magnetic investigation and discussion.

## EXPERIMENTAL SECTION

**Materials and Physical Measurements.** All chemicals were obtained from commercial sources, and they were used without further purification. IR spectra (4000−450 $cm^{-1}$) were obtained in KBr disks on a Perkin-Elmer Spectrum One FT-IR spectrophotometer. Solid-state (diffuse reflectance) electronic spectra were measured as polycrystalline samples on a Perkin-Elmer Lambda2S spectrophotometer, within the range of 450−1100 nm. Elemental analyses were carried out at the Laboratory for Instrumental Analysis, Graduate School of Engineering, Osaka University. The X-ray powder diffraction (XRPD) data were collected on a Rigaku RINT Inplane/ultrax18SAXS-IP diffractometer using monochromatic Cu$K_\alpha$ radiation generated at 40 kV, 200 mA, and the recording speed was 1°/min over the $2\theta$ range of 5−40° at room temperature. All magnetic measurements were performed on polycrystalline samples which were mounted in calibrated gelatin capsules held at the center of a polypropylene straw fixed to the end of the sample rod. The direct current (dc) magnetic measurements were carried out on a Quantum Design MPMS-XL5 SQUID magnetometer equipped with reciprocating sample option (RSO). The alternating current (ac) magnetic measurements were carried out on a Quantum Design MPMS-2 SQUID magnetometer. Magnetic data were corrected for magnetization of the sample holder and for diamagnetic contributions, which were estimated from the Pascal constants.[28]

***Caution!*** *Although not encountered in our experiments, azido compounds are potentially explosive and should be manipulated with special care and used only in small quantities. If possible the hydrothermal method for azido complexes with organic ligands should be avoided.*

**Synthesis of 2D Layer of $[Co(N_3)_2(ampyz)]_n$ (1).** A mixture solution of water (1 mL) and ethanol (2 mL) of $Co(NO_3)_2\cdot 6H_2O$ (0.5 mmol, 145 mg) was carefully layered on an aqueous solution (3 mL) of $NaN_3$ (1 mmol, 65 mg) in a glass vial (20 mL). Then an ethanolic solution (3 mL) of ampyz (1 mmol, 95 mg) was layered on this mixture. The vial was sealed and allowed to stand undisturbed at room temperature. After one week, orange rectangular crystals of **1** were obtained and then washed with water and filtered. It should be mentioned that **1** was obtained in low yield because many small crystals of **1** were eluted with an unidentified pink powder during washing process. Yield 36 mg (30%) based on metal salt. Anal. Calcd for $CoC_4H_5N_9$: C, 20.18; H, 2.12; N, 52.95%. Found: C, 20.62; H, 2.05; N, 53.27%. IR (KBr, $cm^{-1}$): 3407 m, 3326 m, 2100vs, 2080vs, 1629 m, 1541 m, 1443 m, 1354w, 1298w, 1220 m, 1079w, 1025 m, 804 m. UV−vis (diffuse reflectance, $cm^{-1}$): 18400, less than 9000. The single-crystals of **1** were prepared in a U-shaped tube. An ethanolic solution (1 mL) of ampyz (1 mmol) was filled into the one branch of the U-tube that contains distilled water (1 mL). Another branch was filled with an aqueous solution (1 mL) containing $Co(NO_3)_2\cdot 6H_2O$ (0.5 mmol) and $NaN_3$ (1 mmol). After one week, the suitable single-crystals of **1** for X-ray diffraction study were obtained.

**Synthesis of 3D Framework of $[Co(N_3)_2(ampyz)]_n$ (2).** A mixture of $Co(NO_3)_2\cdot 6H_2O$ (0.5 mmol, 145 mg), $NaN_3$ (1 mmol, 65 mg), and ampyz (1 mmol, 95 mg) in water (2 mL) and ethanol (2 mL) was sealed in a Pyrex tube (7 mL), then heated to 90 °C (temperature increase rate of 18 °C/min), allowed to stay for 24 h, and cooled to 30 °C (temperature decrease rate of 0.04 °C/min). The red-orange polygonal crystals of **2** were obtained in a major phase together with unidentified purple powder phase. The crystals were washed with water and filtered to give pure crystals of **2**. Yield 53 mg (45%) based on metal salt. Anal. Calcd for $CoC_4H_5N_9$: C, 20.18; H, 2.12; N, 52.95%. Found: C,19.80; H, 2.15; N, 52.00%. IR (KBr, $cm^{-1}$): 3415 m, 3307 m, 2105vs, 2068vs, 1624 m, 1540 m, 1438 m, 1322w, 1298w, 1218 m, 1026w, 821w. UV−vis (diffuse reflectance, $cm^{-1}$): 18400, 9300.

**X-ray Crystallography and Refinement Details.** All Reflection data were collected on a 1 K Bruker SMART CCD area-detector diffractometer with graphite-monochromated Mo$K\alpha$ radiation ($\lambda$ = 0.71073 Å) using the SMART program.[29] Raw data frame integration was performed with SAINT,[30] which also applied correction for Lorentz and polarization effects. An empirical absorption correction by using the SADABS program[31] was applied. The structure was solved by direct methods and refined by full-matrix least-squares method on $F^2$ with anisotropic thermal parameters for all non-hydrogen atoms using the SHELXTL-PC V 6.1 software package.[32] Hydrogen atoms bound to carbon and nitrogen atoms were placed in calculated positions and refined isotropically with a riding model. Ampyz ligand in **1** lies across two mirror planes so the disordered amino group (N2) was refined with quarter occupancy. The disorder of ampyz is found to be similar to that known for aminopyrazine complexes.[21,22] Therefore, there are many distinct hydrogen bonding networks present via the disordered amino group, and all are symmetry related in which changing one interaction has a knock-on effect. In **1**, the terminal N atoms of EO azido-bridge (N4 and N5) which lie above a mirror plane are disordered, so those atoms were refined with half occupancies. The details of crystal data, selected bond lengths and angles for compounds **1** and **2** are listed in Table 1−3.

## RESULTS AND DISCUSSION

**Syntheses and Characterizations.** The different preparative methods of $Co(NO_3)_2\cdot 6H_2O$, azide anion and ampyz in a 1:2:2 molar ratio in a mixture of ethanol and aqueous media yielded two cobalt(II) coordination polymers containing the ampyz spacer together with the alternating double EO and double EE azido bridging mode which show the different dimensionalities. The layered diffusion reaction in ambient temperature gave the orange rectangular crystals of **1** showing the high symmetric 2D square-grid structure of $[Co(N_3)_2(ampyz)]_n$ whereas the hydrothermal


dx.doi.org/10.1021/ic201035c |*Inorg. Chem.* 2011, 50, 7324–7333

**Table 1. Crystallographic Data for Compounds 1 and 2**

| | 1 | 2 |
|---|---|---|
| formula | $CoC_4H_5N_9$ | $CoC_4H_5N_9$ |
| molecular weight | 238.10 | 238.10 |
| $T$ (K) | 293(2) | 293(2) |
| crystal system | orthorhombic | monoclinic |
| space group | *Immm* | $P2_1/n$ |
| $a$ (Å) | 8.440(2) | 7.3754(15) |
| $b$ (Å) | 7.1808(12) | 14.095(3) |
| $c$ (Å) | 13.845(2) | 7.9773(16) |
| α (deg) | 90.00 | 90.00 |
| $\beta$ (deg) | 90.00 | 97.03(3) |
| $\gamma$ (deg) | 90.00 | 90.00 |
| $V$ (Å$^3$) | 839.1(3) | 823.1(3) |
| $Z$ | 4 | 4 |
| $\rho_{calcd}$ (g cm$^{-3}$) | 1.885 | 1.921 |
| $\mu$ (Mo Kα) (mm$^{-1}$) | 2.019 | 2.058 |
| data collected | 2202 | 9368 |
| unique data | 565 | 1901 |
| $R_1{}^a/wR_2{}^b$ [$I > 2\sigma(I)$] | 0.0397/0.1291 | 0.0285/0.0815 |
| $R_1{}^a/ wR_2{}^b$ [all data] | 0.0493/0.1314 | 0.0296/0.0822 |
| GOF | 1.285 | 1.118 |
| max/min electron density (e Å$^{-3}$) | 0.527/−0.758 | 1.053/−0.330 |

$^a R = \Sigma||F_o| - |F_c||/\Sigma|F_o|$. $^b R_w = \{\Sigma[w(|F_o| - |F_c|)]^2/\Sigma[w|F_o|^2]\}^{1/2}$.

reaction at 90 °C for 1 day yielded the red-orange polygonal crystals of **2** showing 3D framework of $[Co(N_3)_2(ampyz)]_n$. These experiments do not only demonstrate the significant role of the primary units, the excellent azido bridges, and versatile ampyz spacer for building both structures but also demonstrate the important influence of the reaction's conditions on the structural topologies and dimensionalities. The physical purities of crystalline phase of bulk products were confirmed by XRPD technique comparing with their simulated XRD patterns from the single-crystal data (see Supporting Information, Figures S1). The IR spectra of both complexes are quite similar. Complexes **1** and **2** containing both $\mu_2$-1,1 and $\mu_2$-1,3 bridging azides, show two very strong bands due to $\nu_{as}(N_3^-)$ modes at 2100 and 2080 cm$^{-1}$ for **1** and 2105 and 2068 cm$^{-1}$ for **2** indicating the presence of two different azido groups. The weak band at 1322 cm$^{-1}$ is $\nu_s(N_3^-)$ for the EO bridge. This band is not active for the symmetrical EE bridge.[8] Two narrow weak bands in the regions 3400−3300 cm$^{-1}$ can be assigned to $\nu$(N−H) of the primary amine in the ampyz ligand. The solid-state UV−vis diffuse reflectance spectra of both complexes agree with the typical d-d transition of high-spin $Co^{II}$ in octahedral geometry with two observed bands at 20000−18000 and less than 9500 cm$^{-1}$, which are assigned to the $^4T_{1g} \rightarrow {}^4T_{1g}(P)$ and $^4T_{1g} \rightarrow {}^4T_{2g}$ transitions, respectively. The weak band at about 15000 cm$^{-1}$ which is assigned to the $^4T_{1g} \rightarrow {}^4A_{2g}$ transition is not well resolved. The growing bands which appear higher than 22000 cm$^{-1}$ are due to charge transfer transition and internal transition within ampyz[33] (see Supporting Information, Figures S2 and S3).

**Description of the Structures.** *2D Layer of $[Co(N_3)_2(ampyz)]_n$ (**1**).* Compound **1** was crystallized in the orthorhombic crystal system with high centrosymmetric space group, *Immm*. The crystallographic data is shown in Table 1. The coordination environment of the $Co^{II}$ center is shown in Figure 1a. The Co1 atom, EE azido

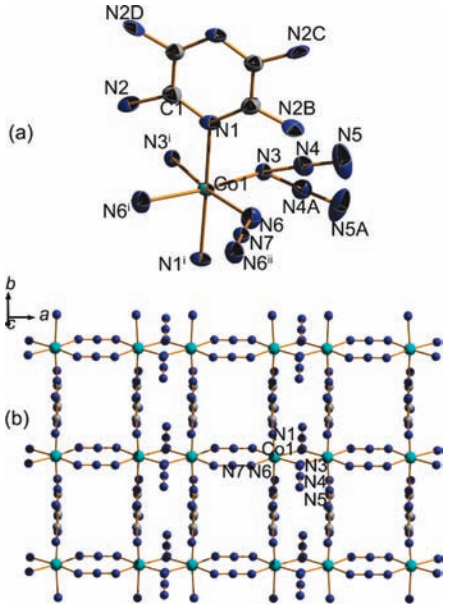


**Figure 1.** (a) Crystal structure and atom labeling scheme of **1**, (i) $x, -y, 2-z$; (ii) $-x, -y, z$. The ellipsoids are shown at 50% probability level. All disordered positions of amino group and N atoms of EO-azide are shown. (b) 2D layer of **1** in the *ab* plane. All H atoms are omitted for clarity.

**Table 2. Selected Bond Lengths (Å) and Angles (deg) for Compound 1**

| Compound 1[a] | | | |
|---|---|---|---|
| Co1−N3 | 2.116(4) | Co1−N6 | 2.141(5) |
| Co1−N3$^i$ | 2.116(4) | Co1−N1$^{iii}$ | 2.193(4) |
| Co1−N6$^{ii}$ | 2.141(5) | Co1−N1 | 2.193(4) |
| N3−Co1−N3$^i$ | 78.3(3) | N6$^{ii}$−Co1−N1$^{iii}$ | 88.10(8) |
| N3−Co1−N6$^{ii}$ | 170.35(19) | N6−Co1−N1$^{iii}$ | 88.10(8) |
| N3$^i$−Co1−N6$^{ii}$ | 92.10(19) | N3−Co1−N1 | 92.24(9) |
| N3−Co1−N6 | 92.10(19) | N3$^i$−Co1−N1 | 92.24(9) |
| N3$^i$−Co1−N6 | 170.35(19) | N6$^{ii}$−Co1−N1 | 88.10(8) |
| N6$^{ii}$−Co1−N6 | 97.5(3) | N6−Co1−N1 | 88.10(8) |
| N3−Co1−N1$^{iii}$ | 92.24(9) | N1$^{iii}$−Co1−N1 | 174.2(2) |
| N3$^i$−Co1−N1$^{iii}$ | 92.24(9) | N6−N7−N6$^{iv}$ | 176.2(8) |
| Co1−N3−Co1$^i$ | 101.7(3) | N5−N4−N3 | 178.1(13) |
| N7−N6−Co1 | 129.3(5) | | |

[a] Symmetry codes: (i) $1-x, -y, 2-z$; (ii) $x, y, 2-z$; (iii) $x, -y, 2-z$; (iv) $-x, -y, z$.

atoms N6, N7 and EO azido N3 atom all lie on a crystallographically *ac* mirror plane. In addition there are three other vertical mirror planes. The first *bc* mirror plane lies on EO azido N3, N4, and N5 atoms. Second is another *bc* mirror plane lying on the EE azido atom N7 and the third is the *ab* mirror plane lying on pyrazine N1 and Co1 atoms. There is only one crystallographically independent $Co^{II}$ ion, which has a slightly elongated octahedron composed of two N atoms from bridging ampyz in the axial sites (2.193(4) Å) and four N atoms from two EE and two EO azide ions located in the equatorial positions (2.141(5)−2.116(4) Å). The selected bond lengths and bond angles are given in Table 2. The adjacent $Co^{II}$ ions are related by those crystallographic mirror planes and inversion center and linked alternately by double EE


dx.doi.org/10.1021/ic201035c |*Inorg. Chem.* 2011, 50, 7324–7333

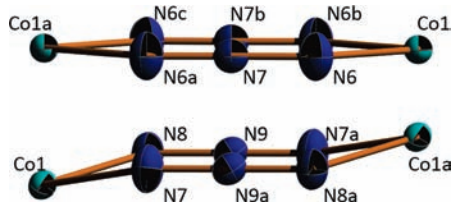


**Figure 2.** Different conformations of the double EE azido bridged Co-($\mu_2$−1,3 $N_3$)$_2$Co ring, complete planarity in **1** (top) and chair conformation in **2** (bottom).

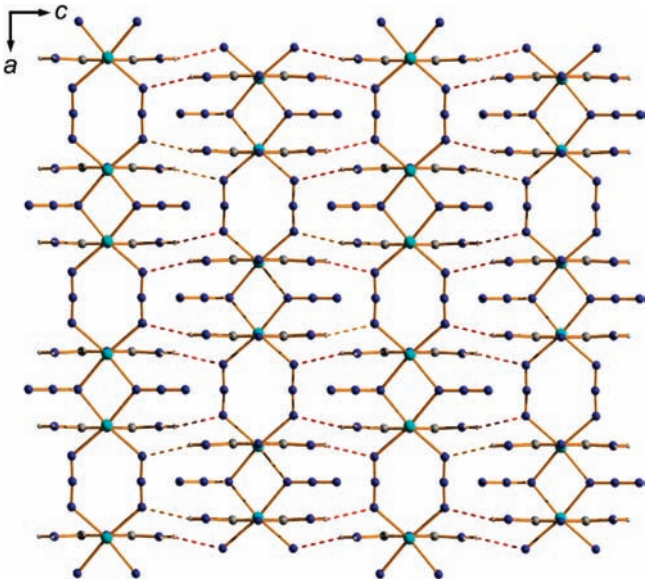


**Figure 3.** Formation of a 3D framework of **1** in the *ac* plane formed by hydrogen bonds between the neighboring layers. The dotted line represents the interlayer N2−H2B···N6 hydrogen bond.

and double EO azido bridges, giving rise to a neutral 1D perfect linear chain along the *a* axis with the Co···Co separations of 5.157(2) and 3.283(1) Å, respectively, where the sum of these values equals to the crystallographic *a* parameter of 8.440(2) Å. In double EO bridged Co($\mu_2$−1,1 $N_3$)$_2$Co moiety, the Co1−N3−Co1A−N3A ring is strictly planar because of the existence of the inversion center and mirror planes with the Co1−N3−Co1A angle of 101.7(3)°, as is usually observed for this kind of azido bridge.[34] The disordered EO azido bridge, which is nearly linear (∠N3−N4−N5 = 178.1°), slightly deviates (up and down) from that plane. For double EE mode, the Co($\mu_2$−1,3 $N_3$)$_2$Co moiety forms the perfect planarity because the crystallographic *ac* mirror plane is placed on this ring. As a result, a dihedral angle $\delta$ between the N6N7N6aN6cN7bN6b mean plane and the CoN6N6b plane is 0°, as shown in Figure 2. The symmetric Co1−N6−N7 angle is 129.3(5)°. It is the uncommon observation of the complete planar for the M($\mu_2$−1,3 $N_3$)$_2$M moiety in the alternating chain of double EE and double EO azido bridges, where the chair conformation is usually observed.[35,36] To our knowledge, the lowest $\delta$ value is 1.82° which is found in [Mn(TaiEt)($N_3$)$_2$]$_n$ (TaiEt = 1-ethyl-2-(*p*-tolylazo)imidazole).[36] The ampyz acts as a *N,N′*-ditopic connector in *trans* position, bridging this neutral azido cobalt(II) chain along the *b* axis and building the 2D square-grid sheet of **1**, as shown in Figure 1b. The intralayer $\pi$−$\pi$ stacking interactions among ampyz spacers stabilize the layer of **1** with the separations of

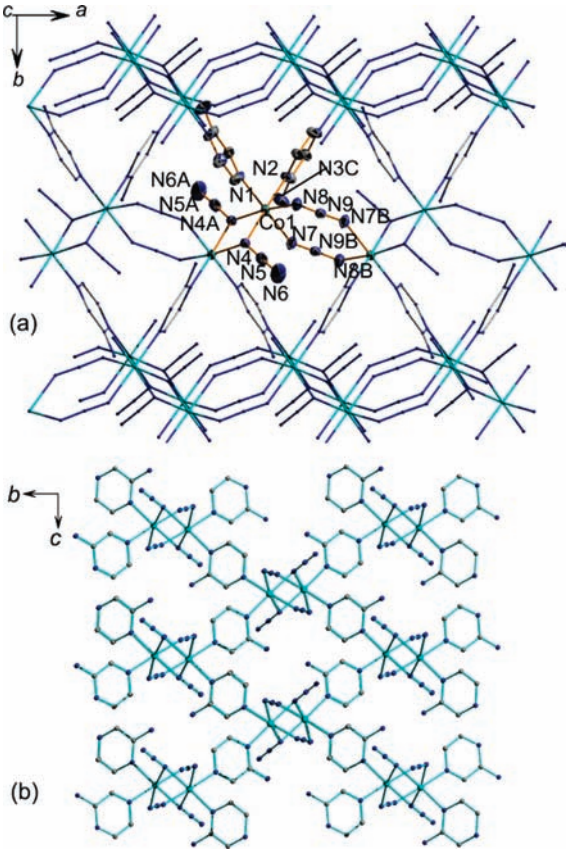


**Figure 4.** (a) 3D framework with atom labeling scheme of **2** in the *ab* plane. The ellipsoids are shown at 50% probability level. Atoms labeled with the notation "A", "B", and "C" are symmetry-generated equivalents, (A) −*x*, 1−*y*, 1−*z*; (B) 1−*x*, 1−*y*, 1−*z*; (C) 1/2+*x*, 1/2−*y*, 1/2+*z*. (b) Another view of 3D structure of **2** in the *bc* plane.

3.502(4) and 4.938(4) Å. The Co···Co separation via the ampyz spacer equals to the crystallographic *b* parameter of 7.1808(12) Å. Moreover, the adjacent 2D sheets of **1** are assembled by interlayer hydrogen bonding between the amine H of ampyz and the N6 atom of the EE azido bridge [N2H···N6$^{i}$ = 2.39 Å (157°), N2···N6$^{i}$ = 3.205(14) Å, (i) =1/2−*x*, 1/2−*y*, 1/2+*z*], yielding a 3D framework of **1** with the closest interlayer Co···Co separation of 7.8453(9) Å, as shown in Figure 3.

*3D Framework of [Co($N_3$)$_2$(ampyz)]$_n$ (**2**).* The crystal structure of **2** is depicted in Figure 4a. Compound **2** shows a 3D framework which is isostructural to the reported zinc(II) compound [Zn($N_3$)$_2$(ampyz)]$_n$.[24] There is one crystallographically independent $Co^{II}$ ion, which is an octahedral $CoN_6$ chromophore composed of two N atoms from two bridging ampyz ligands in *cis*-position and four N atoms from two EE and two EO bridging azide ions. The selected bond lengths and bond angles are given in Table 3. The 3D framework of **2** also consists of an azido cobalt(II) neutral zigzag chain with the alternating double EE and double EO azido bridges along the *a* axis, but *N,N′*-ditopic ampyz spacers link adjacent $Co^{II}$ ions in *cis*-arrangement. The angle of Co···Co···Co in the zigzag chain is 116.62(8)°, and the Co···Co separations via ampyz spacers are 7.1119(14) and 7.6013(14) Å. The hydrogen bonds between the amine H of *cis*-ampyz spacers and N atoms of azido bridges additionally stabilize the entire framework [N3H···N4$^{i}$ = 2.48 Å (138°), N3···N4$^{i}$ = 3.174(3) Å; N3H···N7$^{ii}$ = 2.57 Å (124°), N3···N4$^{ii}$ = 3.130(3) Å; and


dx.doi.org/10.1021/ic201035c |*Inorg. Chem.* 2011, 50, 7324–7333

**Table 3. Selected Bond Lengths (Å) and Angles (deg) for Compound 2**

| Compound 2[a] | | | |
|---|---|---|---|
| Co1−N4$^{i}$ | 2.0986(18) | Co1−N4 | 2.1698(17) |
| Co1−N8 | 2.139(2) | Co1−N7 | 2.1704(19) |
| Co1−N2 | 2.1591(17) | Co1−N1 | 2.1773(17) |
| N4$^{i}$−Co1−N8 | 169.60(7) | N4−Co1−N7 | 87.36(8) |
| N4$^{i}$−Co1−N2 | 98.55(7) | N4$^{i}$−Co1−N1 | 93.31(7) |
| N8−Co1−N2 | 91.82(7) | N8−Co1−N1 | 87.36(7) |
| N4$^{i}$−Co1−N4 | 81.10(7) | N2−Co1−N1 | 90.94(7) |
| N8−Co1−N4 | 88.51(7) | N4−Co1−N1 | 91.47(7) |
| N2−Co1−N4 | 177.58(6) | N7−Co1−N1 | 177.70(7) |
| N4$^{i}$−Co1−N7 | 88.47(7) | N6−N5−N4 | 178.1(3) |
| N8−Co1−N7 | 90.63(7) | N7$^{ii}$−N9−N8 | 176.8(2) |
| N2−Co1−N7 | 90.23(8) | Co1$^{i}$−N4−Co1 | 98.90(7) |

[a] Symmetry codes: (i) $-x$, $1-y$, $1-z$; (ii) $1-x$, $1-y$, $1-z$.

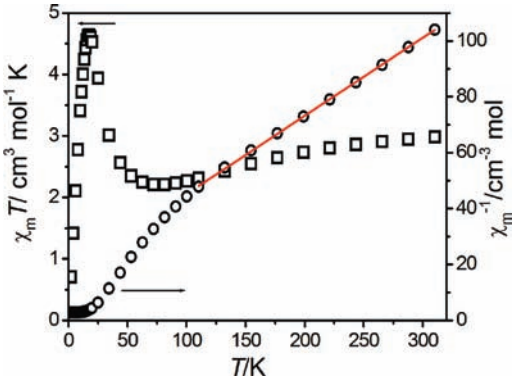


**Figure 5.** Temperature dependence of $\chi_m T$ (□) and $\chi_m^{-1}$ (○) of **1** from 2 to 310 K at $H$ = 10 kOe. The solid lines correspond to the best fit to the Curie−Weiss law.

N3H···N8$^{iii}$ = 2.31 Å (171°), N3···N8$^{iii}$ = 3.165(3) Å, (i) = 1/2+$x$, 1/2−$y$, −1/2+$z$, (ii) = 1/2−$x$, −1/2+$y$, 1/2−$z$, (iii) = −1/2+$x$, 1/2−$y$, 1/2+$z$.]. The adjacent Co$^{II}$ ions in an azido chain are related by inversion centers and linked alternately by double EE and double EO azido bridges with the Co···Co distances of 5.3279(10) Å and 3.2438(6) Å, respectively. In double EO bridging mode, the Co1−N4−Co1A−N4A ring is strictly planar because of the existence of the inversion center with the Co1−N4−Co1A angle of 98.90(7)°. The EO azido bridge is nearly linear (∠N4−N5−N6 = 178.1(3)°) and deviates up and down 43.8° from the plane of $Co_2N_2$. For double EE bridging mode, the EE bridges adopt a chair conformation for the Co($\mu_2$−1,3 $N_3$)$_2$Co unit with the dihedral angle $\delta$ of 12.57(6)°, as shown in Figure 2. The Co1−N8−N9 and Co1−N7−N9B angles are 124.3(2)° and 139.3(2)°, respectively.

**Magnetic Properties.** The magnetic susceptibility of a polycrystalline sample of **1** at 2−310 K is shown in Figure 5. At 310 K, the $\chi_m T$ value is 2.98 cm$^3$ K mol$^{-1}$, which is significantly higher than the spin-only value of 1.87 cm$^3$ K mol$^{-1}$ expected for an $S$ = 3/2 ion, owing to the significant orbital contribution of high-spin Co$^{II}$ in an octahedral surrounding. Upon cooling, the $\chi_m T$ value decreases slowly, attains a minimum value of 2.21 cm$^3$ K mol$^{-1}$ at 70 K, and then shows an abrupt increase to a maximum value of 4.64 cm$^3$ K mol$^{-1}$ at 18 K. This behavior indicates that a small spontaneous magnetization emerges in an antiferromagnetic system, owing to spin canting in which the predominantly antiferromagnetic coupled spins from different sublattices are not perfectly antiparallel, but canting to each other, and the resulting net moments are correlated in a weak ferromagnetic fashion.[5,37,38] Upon further cooling to 2 K, $\chi_m T$ decreases gradually down to 0.70 cm$^3$ K mol$^{-1}$, suggesting antiferromagnetic interactions among the neighboring azido Co$^{II}$ chains or the magnetization saturation. The $\chi_m^{-1}$ values above 100 K were fitted with the Curie−Weiss law $\chi = C/(T - \theta)$ with a Curie constant $C$ = 3.58(2) cm$^3$ K mol$^{-1}$ and a Weiss constant $\theta$ = −61.8(13) K. The $C$ is in the usual range of octahedral high-spin Co$^{II}$ ions.[3,38,39] The negative $\theta$ value can be attributed to both significant spin−orbit coupling of the octahedral Co$^{II}$ ions with a $^4T_{1g}$ ground term and the presence of antiferromagnetic coupling between the Co$^{II}$ centers through the $\mu_{1,3}$-azido bridging ligands. Owing to the lack of a theoretical model for the alternating chain of exchange interactions of octahedral Co$^{II}$ with large spin−orbit coupling effects, the exchange parameters could not be estimated.

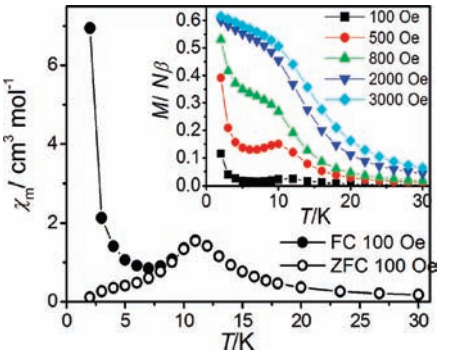


**Figure 6.** ZFC and FC magnetization of **1** at $H$ = 100 Oe from 2 to 30 K. The inset shows the FC magnetization plot of **1** below 30 K at various fields.

To characterize the low-temperature behaviors of **1**, the temperature dependencies of field-cooled (FC) and zero-field-cooled (ZFC) magnetization were performed under a field of 100 Oe upon warming from 2 K, as shown in Figure 6. The ZFC and FC plots present a cusp at around 11 K and show a disagreement below 10 K, suggesting the onset of long-range antiferromagnetic ordering and hysteretic long-range magnetic order, respectively. The temperature dependence of the ac susceptibility measured in a field of 3 Oe shows the same features (Supporting Information, Figures S4). The maximum of $\chi'$ observed at 11 K, in agreement with the above results, confirms the occurrence of a phase transition. The absence of an out-of-phase signal ($\chi''$) around this temperature points to a long-range antiferromagnetic order. However, the $\chi''$ value shows a nonzero signal below 10 K which is the signature of a magnetized state, thus indicating that a partly canted antiferromagnetic structure exists below this temperature.[40−42] The temperature dependence of the FC magnetization of **1** at various fields is depicted in Figure 6, inset. The application of different magnetic fields in the range of 100−3000 Oe showed a strong field dependence of the magnetic susceptibility below $T_N$. For applying fields below 500 Oe, the curves show a swell at around 11 K, indicating the antiferromagnetic ordered state. In the lower temperature region, the magnetizations increase because of small spontaneous magnetization of canted antiferromagnetism. However, applying a magnetic field above 800 Oe is sufficient to

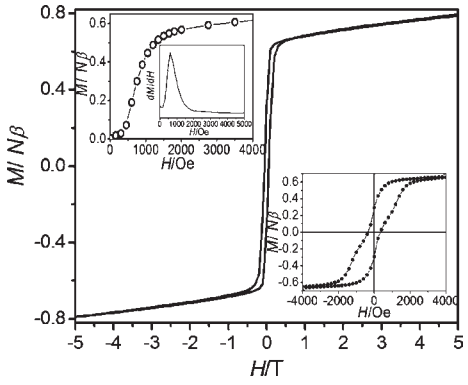


**Figure 7.** Field dependence of the magnetization for **1** at 2 K. The insets show the initial plot in a low field (left) and the hysteresis loop (right).

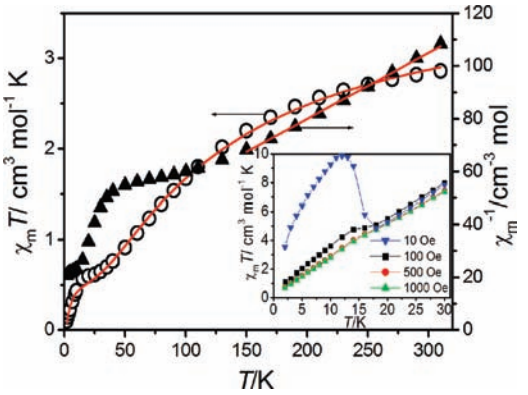


**Figure 8.** Temperature dependence of $\chi_m T$ (○) and $\chi_m^{-1}$ (▲) of **2** from 2 to 310 K at $H$ = 10 kOe. The solid lines correspond to the best fit (see the text). The inset shows the $\chi_m T$ vs $T$ plot of **2** below 30 K at small fields.

overcome these interactions. The cusp disappears, and the magnetization tends to saturate at higher field. These trends suggest a field-induced magnetic phase transition from an antiferromagnetic to a ferromagnetic-like state.[43−45] In addition, the spin canting and metamagnetic-like behaviors were confirmed by the hysteresis loop measurements at 2 K in an external field of 0−5 T, as given in Figure 7. The initial $M(H)$ plot shows a characteristic sigmoidal form (Figure 7, inset), which is a typical feature of a metamagnetic behavior.[18,43−45] The critical field $H_c$ is ≈600 Oe, estimated as the field at which a maximum $\partial M/\partial H$ value is reached. At $H$ < 600 Oe, a linear increase in $M(H)$ is associated with antiferromagnetic interactions, and then above the critical field, the magnetization is drastically increased to $H$ = 5 T without saturation and exhibits a magnetization value of 0.79 $N\beta$, that is far from the theoretical saturation magnetization of $Co^{II}$ ion ($M_s$ = 2.16 $N\beta$, $S'$ = 1/2, $g'$ = 4.33 for octahedral $Co^{II}$ at 2 K),[1,28] suggesting the overall antiferromagnetic coupling between $Co^{II}$ ions. Clearly, a higher field is required to reach saturation to a ferromagnetic phase. Upon decreasing the applied field, the magnetization curve decreases along a different route and exhibits a slightly sigmoid-shaped hysteresis loop with coercive field of ≈350 Oe and remanent magnetization $M_r$ of ≈0.29 $N\beta$. These behaviors confirm the occurrence of spontaneous magnetization of **1** which is in agreement with the observed coexistence of spin-canted antiferromagnetism and metamagnetism. The canting angle (α)[1,5] is estimated to be about 7.7° based on the equation α = $\sin^{-1} M_r/M_s$, where $M_s$ the theoretical saturation magnetization of $Co^{II}$ ion at 2 K. This value is among the big canting angles reported for weak ferromagnets.[5] $[Co(N_3)_2(bpg)_2]$[34] (α = 5.2°), $[Co(N_3)_2(btzb)]$[37] (α = 6.4°), $[Co(N_3)_2(btze)_2]$[37] (α = 9.9°), $[Co_2(N_3)_4(hmta)(H_2O)]$[38] (α = 7.2°), $[Co(N_3)_2$(4-acetylpyridine$)_2]$[46] (α = 15°), $[Fe(N_3)_2(4,4'$-bpy$)]$[47] (α = 7−8°), $[Co($pyrimidine$)_2(X)_2]$ (X = Cl, Br)[48] (α = 9°) and $[Fe($pyrimidine$)_2Cl_2]$[49] (α = 14°).

Temperature dependence of the magnetic susceptibility of **2** at 2−310 K under the field of 10 kOe is presented in Figure 8. The $\chi_m T$ value of 2.86 $cm^3$ K $mol^{-1}$ at 310 K is much higher than the spin-only value of high-spin $Co^{II}$ ions, owing to the orbital contributions of octahedral $Co^{II}$ ions. Upon cooling the temperature, the $\chi_m T$ values decrease gradually and show the cusp around 15 K with the $\chi_m T$ value of 0.57 $cm^3$ K $mol^{-1}$, after that the $\chi_m T$ values drop sharply down to 0.09 $cm^3$ K $mol^{-1}$ at 2 K. The plot of $\chi_m T$ vs $T$ at small fields in the temperature range of 2−30 K is depicted in Figure 8, inset. Below 16 K, the abrupt increases in $\chi_m T$ values are observed under the field below 100 Oe; the susceptibility becomes field dependent. At a small field of 10 Oe, $\chi_m T$ shows an abrupt increase to a maximum value of 9.86 $cm^3$ K $mol^{-1}$ at 12 K before decreasing in the lowest temperature region. The upturn of $\chi_m T$ below 16 K suggests uncompensated magnetic moments of the system arising from spin canting of the antiferromagnetically coupled $Co^{II}$ ions.[26,36] The data above 150 K obeys the Curie−Weiss law with a Curie constant $C$ = 3.99(6) $cm^3$ K $mol^{-1}$ and a Weiss constant $\theta$ = −119(5) K. The $C$ is much larger than the expected spin-only value, which indicates the significant orbital contribution of $Co^{II}$ in an octahedral surrounding.[50] The large negative $\theta$ value suggests the strong spin−orbital coupling of $Co^{II}$ ions in an octahedral field and the antiferromagnetic coupling between $Co^{II}$ ions within 3D framework of **2**. Because of the spin−orbit coupling contribution of $Co^{II}$ ions, it is difficult to find an accurate analytical expression to describe the temperature dependence of the magnetic susceptibility for the polymeric chains of the $Co^{II}$ ions. However, Rueff et al.[51−53] have proposed a very successful phenomenological approach for a low-dimensional antiferromagnetic $Co^{II}$ system that allows an estimation of the strength of the antiferromagnetic exchange interactions and also the effects of spin−orbit coupling. They postulate the phenomenological equation:

$$\chi_m T = A \exp(-E_1/kT) + B \exp(-E_2/kT)$$

$A + B$ equals the Curie constant and $E_1$ and $E_2$ represent the activation energies corresponding to the spin−orbit coupling parameter and the antiferromagnetic exchange interaction, respectively, where $E_2$ is related to the magnetic coupling constant $J$ according to the Ising chain approximation, $\chi_m T \propto \exp(+J/2kT)$. This equation adequately describes the spin−orbit coupling, which results in a splitting between discrete levels and the exponential low-temperature divergence of the susceptibility. The reasonable values for magnetic coupling and spin−orbit interaction have been reported in several studies of 1D and 2D $Co^{II}$ networks.[51,52,54−56] The fitted parameters are $A + B$ = 3.90 $cm^3$ K $mol^{-1}$, practically equivalent to the Curie constant obtained from the Curie−Weiss law in the high temperature range, 3.99 $cm^3$ K $mol^{-1}$. The $E_1/k$ is +112(8) K which is of the same magnitude as those reported for $Co^{II}$ complexes (the order of +100 K).[51,52,54−56]


dx.doi.org/10.1021/ic201035c |Inorg. Chem. 2011, 50, 7324–7333

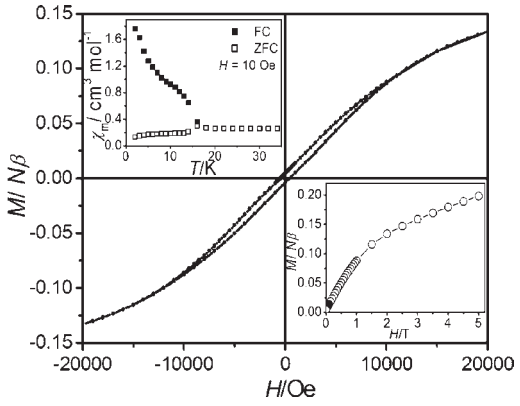


**Figure 9.** Hysteresis curve of **2** at 2 K. The insets show the field dependence of initial magnetization (right) and the ZFC-FC plots of **2** at 10 Oe (left).

For the antiferromagnetic coupling $E_2/k$ = +4.4(2) K, corresponding to $J = -8.8$ K, according to the Ising chain approximation, $\chi_m T \propto \exp(+J/2kT)$. It is noticeable that the small $E_2/k$ value is very close to those reported values for the 2D layer of $[Co(2,2'\text{-bpe})(N_3)_2]_n$ ($E_2/k$ = +4.1(2) K)[27] which contains the same alternating double EO and double EE azido-$Co^{II}$ chain. It is an indication of the overall antiferromagnetic coupling within the 1D azido-$Co^{II}$ chain. However, the $E_1/k$ value of **2** is much higher than that of $[Co(2,2'\text{-bpe})(N_3)_2]_n$ ($E_1/k$ = +61(2) K),[27] implying that **2** presents the stronger spin−orbit coupling of $Co^{II}$ ions in an octahedral field, corresponding to the observation of higher Curie and Weiss constants of **2**.

As a further proof for the presence of the spin canting, the temperature dependencies of the ZFC and the FC magnetization were measured at a low field of 10 Oe, as shown in Figure 9, inset. The obvious divergence of the ZFC and FC plots below 16 K indicates the onset of a magnetized state, which is compatible with the maxima in $\chi'$ and the nonzero $\chi''$ signal at 16 K in the ac susceptibility at 997 Hz, indicative of a long-range magnetic ordering (Supporting Information, Figures S5). The isothermal magnetization with a field up to 5 T at 2 K is depicted in Figure 9. The initial increase of magnetization shows a positive curvature to 0.198 $N\beta$ at 5 T, far from the theoretical saturation magnetization of $Co^{II}$ ion, and no saturation is observed, which is indicative of the overall antiferromagnetic coupling between $Co^{II}$ ions. A hysteresis loop of **2** is clearly observed when the field is less than 1 T, giving a coercive field of ≈450 Oe and remanent magnetization of ≈0.004 $N\beta$. These results indicate that the spin canting effect between overall antiferromagnetically coupled $Co^{II}$ ions leads to residual spins. The canting angle (α) is estimated to be about 0.11° based on the equation $\alpha = \sin^{-1} M_r/M_s$ ($M_s$ = 2.16 $N\beta$ for octahedral $Co^{II}$ at 2 K).

Remarkably, the 2D layer of complex **1** exhibits the coexistence of big canting angle and metamagnetic phenomena whereas the 3D framework of complex **2** only displays the canted antiferromagnetism with a smaller canting angle. As we know that two mechanisms lead to spin canting behavior: (i) single-ion magnetic anisotropy and (ii) antisymmetric exchange interaction.[1,28] However, the spin canted structures are not compatible with both crystal structures of **1** and **2** because of the presence of an inversion center between the bridged $Co^{II}$ sites, which forbids the occurrence of antisymmetric interactions. It is noticeable that the canted antiferromagnets in the presence of an inversion center between metal sites have been often observed in corresponding complexes that contain the 1D chain of alternating double EO and double EE azido-bridged metal(II) ions, as summarized in Table 4. Generally, these complexes were crystallized in low crystal systems (monoclinic and triclinic lattices) and display an inversion center between metal sites. The 1D chain complexes with *cis*-bidentate chelating coligands are widely found in this magnetic system while the 2D layer and 3D framework structures are rarely observed. The isotropic $Mn^{II}$ complexes usually exhibit the overall antiferromagnetic interaction within the 1D alternating ferromagnetic and antiferromagnetic chains, and their magnetostructural correlations have been investigated entirely.[8,35,36,57] Whereas the metamagnetism and weak ferromagnetism due to canted antiferromagnetic system are usually observed in anisotropic ones ($Co^{II}$, $Fe^{II}$, and $Ni^{II}$ complexes).[7,26,27] However some spin canting of 1D $Mn^{II}$ complexes were also reported, which are due to the possible distortion in the crystal structure at low temperature.[36,57,58] Consequently, the observation of spin canting for **1** and **2** should be attributed to the competition of ferromagnetic and antiferromagnetic interactions within intrachain of the alternating double EO and double EE azido bridging mode together with a relevant single-ion anisotropy of octahedral cobalt(II) ions and a possible structure phase transition at low temperature.[7,26,27,36,58] Obviously from the structural data, complex **1** which was crystallized in orthorhombic system with high centrosymmetric space group *Immm* presented the disordered amino group on the ampyz moiety and the disordered terminal EO azido bridge arising from related crystallographic mirror planes and inversion center. We suppose that these disordered positions and inversion centers between the $Co^{II}$ sites somewhere are possibly demolished at very low temperature and develop to the exact atomic location in the crystal lattice with the lower space group. Therefore, the antisymmetric coupling for **1** possibly exists at low temperature together with the single-ion anisotropy of octahedral $Co^{II}$ ion yielding a big canting angle for **1**, as similarly observed in other reported weak ferromagnets with large canting angles.[5,37,38,46,47,59,60] Moreover the interchain and the interlayer weak antiferromagnetic coupling of **1**, which originate from *trans*-ampyz bridging shortly between the azido $Co^{II}$ chain and the interlayer hydrogen bonding between $NH_2$ on ampyz and symmetric double EE azido bridges, would justify the observed maximum of susceptibility at $H_c$ < 600 Oe. In a magnetic field below 600 Oe, the residual magnetic moments due to spin canting on the chains are weak antiferromagnetically coupled to each other (Figure 7, inset). In stronger fields above 600 Oe, the amplitude of the applied magnetic field can overcome the interchain and interlayer weak antiferromagnetic coupling leading to the observed metamagnetic-like behavior of **1**. However, because of the great spin−orbit coupling of $Co^{II}$ ions, the magnetic interaction might be more complicated. Generally, the coexistence of spin canting and metamagnetism is found in the system consisting of a large anisotropy, which leads to a significant spin canting through increasing the possibility of antisymmetric exchange and may induce a metamagnetic transition in the presence of competing interactions within the structure.[40,42,61−65]

It is worthwhile to compare the magnetic properties of **1** and **2** with that of the reported $Co^{II}$ complexes containing similar

**Table 4. Magnetic Properties for the Complexes Containing the Alternating Double EO and Double EE Azido Bridging Mode**

| complex[a] | D | crystal system, space gr. | magnetic behavior[b] | ref. |
|---|---|---|---|---|
| | | *trans*-Monodentate Coligands | | |
| $[Mn(3\text{-Et-4-Mepy})_2(N_3)_2]_n$ | 1D | triclinic, $P\bar{1}$ | overall AF | 66 |
| $[Mn(3\text{-bzpy})_2(N_3)_2]_n$ | 1D | monoclinic, $C2/c$ | overall AF | 9 |
| $[Mn(4\text{-azpy})_2(N_3)_2]_n$ | 1D | triclinic, $P\bar{1}$ | not reported | 67 |
| | | *cis*-Monodentate Coligand | | |
| $[Mn(3,5\text{-lut})_2(N_3)_2]_n$ | 1D | monoclinic, $P2_1/n$ | overall AF | 9 |
| | | *cis*-Bidentate Chelating Coligands | | |
| $[Ni(bpy)(N_3)_2]_n$ | 1D | triclinic, $P\bar{1}$ | C and M | 7 |
| $[Co(bpy)(N_3)_2]_n$ | 1D | triclinic, $P\bar{1}$ | C and M | 7 |
| $[Fe(bpy)(N_3)_2]_n$ | 1D | triclinic, $P\bar{1}$ | C and M | 7 |
| $[Mn(bpy)(N_3)_2]_n$ | 1D | triclinic, $P\bar{1}$ | overall AF | 7,8 |
| $[Mn(bpm)(N_3)_2]_n$ | 1D | monoclinic, $P2_1/n$ | overall AF | 68 |
| $[Ni(dmen)(N_3)_2]_n$ | 1D | monoclinic, $P2_1/n$ | overall AF | 69 |
| $[Ni(aep)(N_3)_2]_n$ | 1D | monoclinic, $P2_1/c$ | overall AF | 69 |
| $[Mn(L^1)(N_3)_2]_n$ | 1D | monoclinic, $P2_1/c$ | overall AF | 35 |
| $[Mn(L^2)(N_3)_2]_n$ | 1D | triclinic, $P\bar{1}$ | overall AF | 35 |
| $[Mn(L^3)(N_3)_2]_n$ | 1D | triclinic, $P\bar{1}$ | overall AF | 35 |
| $[Mn(L^4)(N_3)_2]_n$ | 1D | triclinic, $P\bar{1}$ | overall AF | 35 |
| $[Mn(L^5)(N_3)_2]_n$ | 1D | triclinic, $P\bar{1}$ | overall AF | 35 |
| $[Mn(L^6)(N_3)_2]_n$ | 1D | triclinic, $P\bar{1}$ | overall AF | 70 |
| $[Mn(2\text{-pmp})(N_3)_2]_n$ | 1D | monoclinic, $C2/c$ | overall AF | 71 |
| $[Mn(taiEt)(N_3)_2]_n$ | 1D | triclinic, $P\bar{1}$ | C ($T_c$= 40 K) | 36 |
| $[Mn(dpq)(N_3)_2]_n$ | 1D | triclinic, $P\bar{1}$ | C ($T_c$= 6 K) | 58 |
| $[Mn(dpa)(N_3)_2]_n$ | 1D | monoclinic, $P2_1/c$ | C ($T_c$= 15 K) | 57 |
| $[Co(dpa)(N_3)_2]_n$ | 1D | monoclinic, $P2_1/n$ | C ($T_c$= 12.4 K) | 26 |
| | | *trans*-Bidentate Bridging Coligands | | |
| $[Mn(L^7)(N_3)_2]_n$ | 2D | triclinic, $P\bar{1}$ | overall AF | 72 |
| $[Co(2,2'\text{-bpe})(N_3)_2]_n$ | 2D | triclinic, $P\bar{1}$ | C ($T_c$= 12 K) | 27 |
| $[Co(ampyz)(N_3)_2]_n$ (**1**) | 2D | orthorhombic, *Immm* | C and M ($T_c$= 10 K) | this work |
| | | *cis*-Bidentate Bridging Coligand | | |
| $[Co(ampyz)(N_3)_2]_n$ (**2**) | 3D | monoclinic, $P2_1/n$ | C ($T_c$= 16 K) | this work |

[a] Abbreviations: 3-Et-4-Mepy =3-ethyl-4-methylpyridine, 3-bzpy =3-benzoylpyridine, 4-azpy =4-azidopyridine, 3,5-lut =3,5-dimethylpyridine, bpy =2,2′-bipyridine, bpm = bis(pyrazol-1-yl)methane, dmen = *N*,*N*-dimethylethylenediamine, aep =2-aminoethylpyridine, $L^1$ = *N*-phenyl-2-carbaldimine, $L^2$ = *N*-(*p*-tolyl)-2-carbaldimine, $L^3$ = *N*-(*m*-tolyl)-2-carbaldimine, $L^4$ = *N*-(*p*-chlorophenyl)2-carbaldimine, $L^5$ = *N*-(*m*-chlorophenyl)-2-carbaldimine, $L^6$ = *N*-(2-pyridylmethylene)octylamine, $L^7$= *N*,*N*′-Bis-(1-pyridin-3-yl-ethylidene) hydrazine, 2-pmp =2-(pyrazol-1-ylmethyl)pyridine, taiEt = 1-ethyl-2-(*p*-tolylazo)-imidazole, dpq = dipyrido-(3,2-d:2′,3′-f)-quinoxaline, dpa =2,2′-dipyridylamine, and 2,2′-bpe =1,2-bis(2-pyridyl)ethylene. [b] Abbreviations: C = canted antiferromagnetism, M= metamagnetism, and AF = antiferromagnetism.

alternating double EO and double EE azido bridging mode, as shown in Table 5. The comparison demonstrates that all compounds are hard magnets at 2 K ($H_c \approx 300-500$ Oe) and only complex **1** which is in the highest-symmetry space group, shows the coexistence of big spin canting angle and metamagnetism whereas the others display very small spin canting angle. This unusual feature of **1** could be attributed to the above-mentioned significant antisymmetric exchange interaction between $Co^{II}$ ions and the single-ion anisotropy of $Co^{II}$ ion. In addition, the interlayer hydrogen bonding between $NH_2$ of ampyz and symmetric double EE azido bridges in **1** which are not found in other structures, might play the important role on the presence of the field-induced metamagnetic phase transition. In comparison with **1**, complex **2** and the others which were crystallized in lower crystal systems reveal very small canting angles. This result indicates that the major magnetic anisotropy of octahedral $Co^{II}$ ion in **2** plays a key role on spin canting as well as a minor magnitude of antisymmetric coupling between $Co^{II}$ ions which possibly arises from a distortion in the crystal framework, suppressing the inversion center at low temperature. The above-mentioned complex **2** shows the very close antiferromagnetic coupling $E_2/k$ value to that reported for $[Co(2,2'\text{-bpe})(N_3)_2]_n$ but the Weiss constant and $E_1/k$ value are much higher, which point to the very strong spin−orbital coupling of octahedral $Co^{II}$ ions of **2**. This extra inherent anisotropy of the $Co^{II}$ ions for **2** might provide an additional contribution to a larger degree of spin canting, resulting in the observation of the higher $M_r$ and the larger canting angle when comparing with $[Co(2,2'\text{-bpe})(N_3)_2]_n$ and $[Co(dpa)(N_3)_2]_n$. The $T_N$ of **2** is slightly higher than other complexes owing to the closest Co···Co distance among the magnetic chains in 3D covalent framework of **2**.


dx.doi.org/10.1021/ic201035c |*Inorg. Chem.* 2011, 50, 7324–7333

Table 5. Structural and Magnetic Data for $Co^{II}$ Complexes Containing the Alternating Double EO and Double EE Azido Bridging Mode

| | compound[a] | | | |
|---|---|---|---|---|
| | **1** | **2** | $[Co(2,2'\text{-bpe})(N_3)_2]_n$ | $[Co(dpa)(N_3)_2]_n$ |
| dimension | 2D | 3D | 2D | 1D |
| co-ligand | *trans*-bridging | *cis*-bridging | *trans*-bridging | *cis*-chelating |
| crystal system | orthorhombic | monoclinic | triclinic | monoclinic |
| space group | *Immm* | $P2_1/n$ | $P\bar{1}$ | $P2_1/n$ |
| Co−N−Co (deg) | 101.7(3) | 98.90(7) | 102.25(14) | 103.7 |
| $\delta$ (deg) [b] | 0 | 12.57(6) | 33.8(1) | 36.0 |
| Co···Co (Å) [c] | 7.1808(12) | 7.1119(14) | 8.322(2) | 9.294 |
| magnetic behavior | canted AF, metamagnetism | canted AF | canted AF | canted AF |
| $\theta$ (K) | −61.8(13)[d] | −119(5)[d] | −58(2)[d] | −40.0[e] |
| $T_N$ (K) | 10 | 16 | 12 | 12.4 |
| $M_r$ ($N\beta$) [f] | 0.29 | 0.004 | 0.002 | 0.002 |
| $H_c$ (Oe) [g] | 350 | 450 | 300 | 500 |
| $\alpha$ (deg) [h] | 7.7 | 0.11 | 0.05 | 0.05 |
| ref. | this work | this work | 27 | 26 |

[a] Abbreviations: 2,2′-bpe = 1,2-bis(2-pyridyl)ethylene and dpa = 2,2′-dipyridylamine. [b] The dihedral angle between the mean plane of $Co(\mu_2\text{-}1,3\ N_3)_2Co$ and the Co−N−N plane. [c] The shortest Co···Co distance among alternating double EO and double EE azido-$Co^{II}$ chain. [d] The best fit to Curie−Weiss law above 150 K. [e] The best fit to Curie−Weiss law above 210 K. [f] Remanent magnetization at 2 K. [g] Coercive field at 2 K. [h] Canting angle based on the equation $\alpha = \sin^{-1} M_r/M_s$ ($M_s$ = 2.16 $N\beta$).

## CONCLUSIONS

By using the versatile ampyz spacer, two high dimensional cobalt(II) azido inorganic−organic hybrid frameworks, which contain similarly alternating double EO and double EE azido-bridged $Co^{II}$ chains, were obtained from the different preparative methods. The high symmetric square-grid structure of **1** from the layer diffusion method, which consists of *trans*-ampyz bridging between octahedral $Co^{II}$ centers in axial positions, presents the coexistence of a big spin canting angle and metamagnetism below 10 K. The canting angle is estimated to be 7.7°, and the critical field for metamagnetic phase transition is ≈600 Oe at 2 K. The interlayer hydrogen bonding between the amino group of the ampyz spacer and the symmetric double EE azido bridges plays an important role in the field-induced metamagnetic phase transition. The spin canting of **1** could be attributed to the significant antisymmetric exchange arising from the structure phase transition at low temperature and the great role of magnetic anisotropy of the $Co^{II}$ ion. Whereas the 3D framework containing the *cis*-ampyz bridging among $Co^{II}$ centers of **2** was synthesized from the hydrothermal technique, it was crystallized in a lower space group and exhibited only small spin-canted antiferromagnetism below 16 K. It suggests that the large magnetic anisotropy in **2** might contribute a spin canting together with small antisymmetric coupling between $Co^{II}$ ions, arising from a distortion in the crystal net at low temperature, which is frequently found in the related complexes containing the same bridging mode of the azide. These results provide a motivation for future investigations and demonstrate the importance of the crystal engineering of inorganic−organic hybrid framework in the field of molecular-based magnetic materials.

## ASSOCIATED CONTENT

**Supporting Information.** X-ray crystallographic information files (CIF) for **1**−**2** (CCDC nos. 823144 and 823145), IR and UV−vis spectra, XRPD patterns, and additional magnetic data. This material is available free of charge via the Internet at http://pubs.acs.org.

## AUTHOR INFORMATION

### Corresponding Author

*E-mail: sujittra@kku.ac.th. Fax: +66-43-202-373.

## ACKNOWLEDGMENT

Funding for this work is provided by The Thailand Research Fund (Grant BRG5280012), the Royal Golden Jubilee Ph.D. Program of The Thailand Research Fund (Grant PHD/0019/2549), the Higher Education Research Promotion and National Research University Project of Thailand, Office of the Higher Education Commission, through the Advanced Functional Materials Cluster of Khon Kaen University and the Center of Excellence for Innovation in Chemistry (PERCH−CIC), Commission on Higher Education, Ministry of Education, Thailand. The support of JSPS Exchange Program for East Asian Young Researchers 2008-2009 and Osaka University are also gratefully acknowledged.

## REFERENCES

(1) Kahn, O. *Molecular Magnetism*; VCH: New York, 1993.
(2) Miller, J. S. *Inorg. Chem.* **2000**, *39*, 4392.
(3) Kurmoo, M. *Chem. Soc. Rev.* **2009**, *38*, 1353.
(4) Dechambenoit, P.; Long, J. R. *Chem. Soc. Rev.* **2011**, *40*, 3249.
(5) Weng, D.-F.; Wang, Z.-M.; Gao, S. *Chem. Soc. Rev.* **2011**, *40*, 3157.
(6) Zeng, Y.-F.; Hu, X.; Liu, F.-C.; Bu, X.-H. *Chem. Soc. Rev.* **2009**, *38*, 469.
(7) Viau, G.; Lombardi, M. G.; Munno, G. D.; Julve, M.; Lloret, F.; Faus, J.; Caneschic, A.; Clemente-Juana, J. M. *Chem. Commun.* **1997**, 1195.
(8) Cortés, R.; Drillon, M.; Solans, X.; Lezama, L.; Rojo, T. *Inorg. Chem.* **1997**, *36*, 677.

(9) Abu-Youssef, M. A. M.; Escuer, A.; Gatteschi, D.; Goher, M. A. S.; Mautner, F. A.; Vicente, R. *Inorg. Chem.* **1999**, *38*, 5716.
(10) Liu, F.-C.; Zeng, Y.-F.; Zhao, J.-P.; Hu, B.-W.; Bu, X.-H.; Ribas, J.; Cano, J. *Inorg. Chem.* **2007**, *46*, 1520.
(11) Martín, S.; Barandika, M. G.; Lezama, L.; Pizarro, J. L.; Serna, Z. E.; Larramendi, J. I. R. d.; Arriortua, M. I.; Rojo, T.; Cortés, R. *Inorg. Chem.* **2001**, *40*, 4109.
(12) Abu-Youssef, M. A. M.; Drillon, M.; Escuer, A.; Goher, M. A. S.; Mautner, F. A.; Vicente, R. *Inorg. Chem.* **2000**, *39*, 5022.
(13) Escuer, A.; Aromí, G. *Eur. J. Inorg. Chem.* **2006**, 4721.
(14) Wang, X.-Y.; Wang, Z.-M.; Gao, S. *Chem. Commun.* **2008**, 281.
(15) Adhikarya, C.; Koner, S. *Coord. Chem. Rev.* **2010**, *254*, 2933.
(16) Abu-Youssef, M. A. M.; Escuer, A.; Mautnerc, F. A.; Öhrström, L. *Dalton Trans.* **2008**, 3553.
(17) Massoud, A. a. A.; Abu-Youssef, M. A. M.; Vejpravová, J. P.; Langera, V.; Öhrström, L. *CrystEngComm* **2009**, *11*, 223.
(18) Hao, X.; Wei, Y.; Zhang, S. *Chem. Commun.* **2000**, 2271.
(19) Manson, J. L.; Arif, A. M.; Miller, J. S. *Chem. Commun.* **1999**, 1479.
(20) Dong, W.; Ouyang, Y.; Liao, D.-Z.; Yan, S.-P.; Cheng, P.; Jiang, Z.-H. *Inorg. Chim. Acta* **2006**, *359*, 3363.
(21) Boonmak, J.; Youngme, S.; Chaichit, N.; van Albada, G. A.; Reedijk, J. *Cryst. Growth Des.* **2009**, *9*, 3318.
(22) Boonmak, J.; Nakano, M.; Chaichit, N.; Pakawatchai, C.; Youngme, S. *Dalton Trans.* **2010**, *39*, 8161.
(23) Manson, J. L.; Schlueter, J. A.; Geiser, U.; Stone, M. B.; Reich, D. H. *Polyhedron* **2001**, *20*, 1423.
(24) Goher, M. A. S.; Mautner, F. A.; Sodin, B.; Bitschnau, B. *J. Mol. Struct.* **2008**, *879*, 96.
(25) Tronic, T. A.; DeKrafft, K. E.; Mi, J. L.; Ley, A. N.; Pike, R. D. *Inorg. Chem.* **2007**, *46*, 8897.
(26) Wang, X.-T.; Wang, X.-H.; Wang, Z.-M.; Gao, S. *Inorg. Chem.* **2009**, *48*, 1301.
(27) Boonmak, J.; Nakano, M.; Youngme, S. *Dalton Trans.* **2011**, *40*, 1254.
(28) Carlin, R. L. *Magnetochemistry*; Springer-Verlag: Berlin, Germany, 1986.
(29) *SMART 5.6*; Bruker AXS Inc.: Madison, WI, 2000.
(30) *SAINT 4.0 Software Reference Manual*; Siemens Analytical X-Ray Systems Inc.: Madison, WI, 2000.
(31) Sheldrick, G. M. *SADABS, Program for Empirical Absorption correction of Area Detector Data*; University of Göttingen: Göttingen, Germany, 2000.
(32) Sheldrick, G. M. *Acta Crystallogr.* **2008**, *A64*, 112.
(33) Lever, A. B. P. *Inorganic Electronic Spectroscopy*, 2 ed.; Elsevier: Amsterdam, The Netherlands, 1984.
(34) Wang, X.-Y.; Wang, L.; Wang, Z.-M.; Gao, S. *J. Am. Chem. Soc.* **2006**, *128*, 674.
(35) Gao, E.-Q.; Bai, S.-Q.; Yue, Y.-F.; Wang, Z.-M.; Yan, C.-H. *Inorg. Chem.* **2003**, *42*, 3642.
(36) Umasankar, R.; Sk, J.; Barindra Kumar, G.; Montserrat, M.; Joan, R.; Golam, M.; Tian -Huey, L.; Chittaranjan, S. *Eur. J. Inorg. Chem.* **2004**, 250.
(37) En-Qing, G.; Pei-Pei, L.; Yan-Qin, W.; Qi, Y.; Qing-Lun, W. *Chem.—Eur. J.* **2009**, *15*, 1217.
(38) Mautner, F. A.; Öhrström, L.; Sodin, B.; Vicente, R. *Inorg. Chem.* **2009**, *48*, 6280.
(39) Yoo, H. S.; Kim, J. I.; Yang, N.; Koh, E. K.; Park, J.-G.; Hong, C. S. *Inorg. Chem.* **2007**, *46*, 9054.
(40) Zeng, M.-H.; Zhang, W.-X.; Sun, X.-Z.; Chen, X.-M. *Angew. Chem., Int. Ed.* **2005**, *44*, 3079.
(41) Huang, Z.-L.; Drillon, M.; Masciocchi, N.; Sironi, A.; Zhao, J.-T.; Rabu, P.; Panissod, P. *Chem. Mater.* **2000**, *12*, 2805.
(42) Yang, B.-P.; Prosvirin, A. V.; Guo, Y.-Q.; Mao, J.-G. *Inorg. Chem.* **2008**, *47*, 1453.
(43) Winter, S. M.; Cvrkalj, K.; Dube, P. A.; Robertson, C. M.; Probert, M. R.; Howard, J. A. K.; Oakley, R. T. *Chem. Commun.* **2009**, 7309.
(44) Pasán, J.; Sanchiz, J. n.; Ruiz-Pérez, C.; Campo, J.; Lloret, F.; Julve, M. *Chem. Commun.* **2006**, 2857.
(45) Sun, W.-W.; Tian, C.-Y.; Jing, X.-H.; Wang, Y.-Q.; Gao, E.-Q. *Chem. Commun.* **2009**, 4741.
(46) Wang, X.-Y.; Wang, Z.-M.; Gao, S. *Inorg. Chem.* **2008**, *47*, 5720.
(47) Fu, A.; Huang, X.; Li, J.; Yuen, T.; Lin, C. L. *Chem.—Eur. J.* **2002**, *8*, 2239.
(48) Nakayama, K.; Ishida, T.; Takayama, R.; Hashizume, D.; Yasui, M.; Iwasaki, F.; Nogami, T. *Chem. Lett.* **1998**, 497.
(49) Feyerherm, R.; Loose, A.; Ishida, T.; Nogami, T.; Doll, K. *Phys. Rev. B* **2004**, *69*, 134427.
(50) Li, R.-Y.; Wang, X.-Y.; Liu, T.; Xu, H.-B.; Zhao, F.; Wang, Z.-M.; Gao, S. *Inorg. Chem.* **2008**, *47*, 8134.
(51) Rueff, J. M.; Masciocchi, N.; Rabu, P.; Sironi, A.; Skoulios, A. *Eur. J. Inorg. Chem.* **2001**, 2843.
(52) Rueff, J. M.; Masciocchi, N.; Rabu, P.; Sironi, A.; Skoulios, A. *Chem.—Eur. J.* **2002**, *8*, 1813.
(53) Rabu, P.; Rueff, J. M.; Huang, Z. L.; Angelov, S.; Souletie, J.; Drillon, M. *Polyhedron* **2001**, *20*, 1677.
(54) Manna, S. C.; Konar, S.; Zangrando, E.; Okamoto, K.-i.; Ribas, J.; Chaudhuri, N. R. *Eur. J. Inorg. Chem.* **2005**, 4646.
(55) Keene, T. D.; Hursthouse, M. B.; Price, D. J. *Cryst. Growth Des.* **2009**, *9*, 2604.
(56) Liu, F.-C.; Zeng, Y.-F.; Jiao, Bu, X.-H.; Ribas, J.; Batten, S. R. *Inorg. Chem.* **2006**, *45*, 2776.
(57) Villanueva, M.; Mesa, J.; Urtiaga, M. K.; Cortés, R.; Lezama, L.; Arriortua, M. a. I.; Rojo, T. *Eur. J. Inorg. Chem.* **2001**, 1581.
(58) Zhang, J.-Y.; Liu, C.-M.; Zhang, D.-Q.; Gao, S.; Zhu, D.-B. *Inorg. Chem. Commun.* **2007**, *10*, 897.
(59) Palii, A. V.; Reu, O. S.; Ostrovsky, S. M.; Klokishner, S. I.; Tsukerblat, B. S.; Sun, Z.-M.; Mao, J.-G.; Prosvirin, A. V.; Zhao, H.-H.; Dunbar, K. R. *J. Am. Chem. Soc.* **2008**, *130*, 14729.
(60) Lappas, A.; Wills, A. S.; Green, M. A.; Prassides, K.; Kurmoo, M. *Phys. Rev. B* **2003**, *67*, 144406.
(61) Wang, X.-Y.; Wang, L.; Wang, Z.-M.; Su, G.; Gao, S. *Chem. Mater.* **2005**, *17*, 6369.
(62) Mitsumoto, K.; Shiga, T.; Nakano, M.; Nihei, M.; Nishikawa, H.; Oshio, H. *Eur. J. Inorg. Chem.* **2008**, 4851.
(63) Ko, H. H.; Lim, J. H.; Kim, H. C.; Hong, C. S. *Inorg. Chem.* **2006**, *45*, 8847.
(64) Jia, H.-P.; Li, W.; Ju, Z.-F.; Zhang, J. *Chem. Commun.* **2008**, 371.
(65) Humphrey, S. M.; Wood, P. T. *J. Am. Chem. Soc.* **2004**, *126*, 13236.
(66) Abu-Youssef, M. A. M.; Escuer, A.; Goher, M. A. S.; Mautner, F. A.; Vicente, R. *Eur. J. Inorg. Chem.* **1999**, 687.
(67) Mautner, F. A.; Egger, A.; Sodin, B.; Goher, M. A. S.; Abu-Youssef, M. A. M.; Massoud, A.; Escuer, A.; Vicente, R. *J. Mol. Struct.* **2010**, *969*, 192.
(68) Tang, L.-F.; Zhang, L.; Li, L.-C.; Cheng, P.; Wang, Z.-H.; Wang, J.-T. *Inorg. Chem.* **1999**, *38*, 6326.
(69) Monfort, M.; Resino, I.; Ribas, J.; Solans, X.; Font-Bardia, M.; Rabu, P.; Drillon, M. *Inorg. Chem.* **2000**, *39*, 2572.
(70) Bai, S.-Q.; Gao, E.-Q.; He, Z.; Fang, C.-J.; Yue, Y.-F.; Yan, C.-H. *Eur. J. Inorg. Chem.* **2006**, 407.
(71) Gao, E.-Q.; Bai, S.-Q.; Wang, C.-F.; Yue, Y.-F.; Yan, C.-H. *Inorg. Chem.* **2003**, *42*, 8456.
(72) Gao, E.-Q.; Cheng, A.-L.; Xu, Y.-X.; He, M.-Y.; Yan, C.-H. *Inorg. Chem.* **2005**, *44*, 8822.